Speed-up, slowdown, and redirection of ice flow on neighbouring ice streams in the Pope, Smith and Kohler region of West Antarctica

Heather L. Selley[1], Anna E. Hogg[1], Benjamin J. Davison[1], Pierre Dutrieux[2], Thomas Slater[3].

[1]School of Earth and Environment, University of Leeds, UK.

5   [2]British Antarctic Survey, UK.

[3]Department of Geography and Environmental Sciences, Centre for Polar Observation and Modelling, Northumbria University, Newcastle-Upon-Tyne NE1 8ST, UK.

Correspondence to: Heather L. Selley (H.L.Selley@leeds.ac.uk)

10   **Abstract.**

The ice streams feeding Dotson and Crosson Ice Shelves are some of the fastest changing in West Antarctica. We use satellite observations to measure the change in ice speed and flow direction on eight ice streams in the Pope, Smith and Kohler region of West Antarctica from 2005 to 2022. Seven ice streams have sped up at the grounding line, with the largest increase in ice

15   speed at Smith West Glacier (87 %) whilst Kohler West Glacier has slowed by 10 %. We observe progressive redirection of ice flowlines from Kohler West into the more rapidly thinning and accelerating Kohler East Glacier, resulting in the deceleration of Kohler West Glacier and eastward migration of the ice divide between Dotson and Crosson Ice Shelves. These observations reveal previously undocumented impacts of spatially varying ice speed and thickness changes on flow direction and ice flux into downstream ice shelves, which may influence ice shelf and sheet mass change during the 21st century.

20   **1 Introduction**

Ice loss from Antarctica is dominated by increased grounding line discharge from ice streams draining into the Amundsen Sea Embayment (ASE) from the West Antarctic Ice Sheet (WAIS) (Joughin et al., 2010; Rignot et al., 2008, 2019; Shepherd et al., 2012, 2018). Combined, the ice streams in the ASE – Pine Island, Thwaites, Haynes, Pope, Smith, and Kohler Glaciers - contain 1.2 m of sea level rise potential (Morlighem et al., 2011; Mouginot et al., 2014), and are theoretically susceptible to

25   Marine Ice Sheet Instability (MISI) due to being grounded on predominantly retrograde bed topography (Favier et al., 2014; Joughin et al., 2014; Schoof, 2007; Weertman, 1974). Across the ASE, satellite observations have shown widespread grounding line retreat (Konrad et al., 2018; Milillo et al., 2022; Scheuchl et al., 2016), thinning (Konrad et al., 2017; Pritchard et al., 2012; Rignot et al., 2019; Shepherd et al., 2018) and acceleration (Mouginot et al., 2014) since at least the early 1970's. It is likely these ice dynamic changes initiated in or before the 1940's, particularly on Pine Island Glacier (Davies et al., 2017;

30   Rignot et al., 2014; Shepherd et al., 2019; Smith et al., 2016). While Ice loss from Pine Island and Thwaites Glaciers dominate the overall mass balance of the ASE, observations show that 21st century rates of thinning and acceleration at Pope, Smith, and Kohler (PSK) Glaciers have so far been proportionally faster and larger than that of their neighbours (Davison et al., 2023; Konrad et al., 2017; McMillan et al., 2014; Mouginot et al., 2014; Rignot et al., 2014; Surawy-Stepney et al., 2023b). Ice speed

and grounding line discharge at Pope, Smith, and Kohler East Glaciers (Fig. 1) more than doubled between the 1970s and 2010

35   (Mouginot et al., 2014; Rignot et al., 2016). Smith Glacier thinned by up to 9 m/yr between 2010 and 2013 (McMillan et al.,
2014), and its grounding line has retreated at speeds of up to 2 km/yr (Konrad et al., 2018) - the fastest rate recorded in
Antarctica during the satellite era.

The PSK region contains 8 distinct ice streams, two of which have dual branches extending ~100 km inland (Fig. 1). Haynes,

40   Vane, Pope, Smith East, Smith West, and Kohler East Glaciers flow into the Crosson Ice Shelf, whereas Kohler West and
Horrall Glaciers flow into the Dotson Ice Shelf (Fig. 1). Parts of Crosson Ice Shelf have doubled in speed, comparable to the
grounded upstream areas that now flow at speeds of ~1.2 km/yr, and the ice shelf has extensive rifting, particularly on its
eastern side (Lilien et al., 2018; Mouginot et al., 2014) (Fig. 1). Both Dotson and Crosson Ice Shelves have thinned (Pritchard
et al., 2012) by 10 % and 18 % (Paolo et al., 2015) respectively between 1994 and 2012, with average basal melt rates of 5.4

45   $\pm$ 1.6 and 7.8 $\pm$ 1.8 m/yr (Adusumilli et al., 2020), respectively. Kohler West Glacier and the Dotson Ice Shelf into which it
flows have changed less over the last 30 years, which has been attributed to the prograde bed slope on which Kohler West
Glacier rests (Milillo et al., 2022; Scheuchl et al., 2016). Satellite observations show that the grounding line of Kohler West
Glacier has retreated by a more modest 200 m/yr between 1992 to 2011 (Milillo et al., 2022), with no change in ice speed
observed since 2015 (Scheuchl et al., 2016) despite the ice shelf thinning near the grounding line (Gourmelen et al., 2017;

50   Zinck et al., 2023). Despite the importance of the PSK region, due to its contemporary and potential contribution to sea level
rise, the spatial pattern of its speed change is not well characterised since 2015, and the consequences for coupled ice shelf-ice
sheet dynamics are not adequately understood.

In this study, we combine new high-resolution satellite observations with existing measurements of ice velocity from PSK

55   over 17.5 years up to 2022, to extend the record of ice speed and investigate the impact of spatially varying acceleration and
thinning on ice flow direction and ice flux into Crosson and Dotson ice shelves. We measure the calving front location on
Dotson and Crosson Ice Shelves from 2005 to 2020 to examine the impact of ice sheet velocity change on these two important
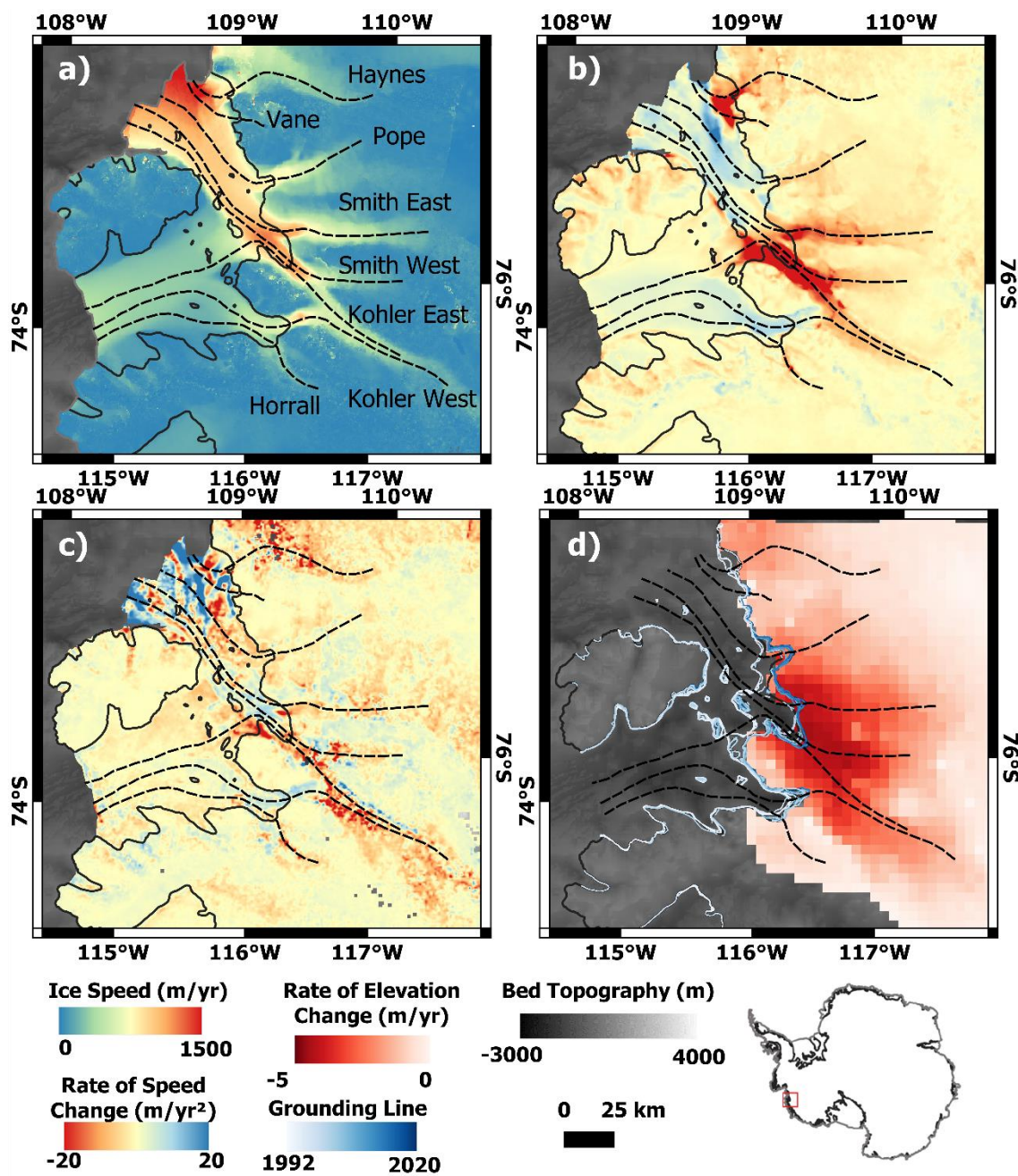Antarctic ice shelves.

60

Figure 1: Ice speed and rate of speed change at Haynes, Vane, Pope, Smith East, Smith West, Kohler East, Kohler West and Horrall Glaciers, which feed the Crosson and Dotson Ice Shelves in the Amundsen Sea Sector of West Antarctica. (A) Average 2015 to 2022 ice speed over the PSK region, measured using interferometric Wide (IW) mode synthetic aperture radar (SAR) data acquired by the Sentinel-1a/b satellites. The 2011 grounding line location (solid black line) (Rignot et al., 2016) and the location of the 8 flow line profiles (dashed black lines) are also shown. **(B)** Observed rate of speed change over the full 15-year study period, from 2005.05.01 to 2020.05.30. **(C)** Observed rate of speed change during the Sentinel-1 period from 2015.06.01 to 2020.05.31. Measurements are superimposed on BedMachine bedrock topography (Morlighem et al., 2017). **(D)** Rate of elevation change for 1992 to 2023 (red) (Shepherd et al., 2019) and grounding line locations from 1992 to 2020 (blue) (Milillo et al., 2022; Rignot et al., 2016).

2 Method

2.1 Ice Velocity Measurements

We measured the ice speed of Haynes, Vane, Pope, Smith, Kohler, and Horrall Glaciers from January 2015 to December 2022 using Sentinel-1a and -1b synthetic aperture radar (SAR) satellite imagery (Table S2). Ice velocity was measured using the intensity feature tracking technique which measures the displacement of visible features at or near to the ice surface such as crevasses, rifts and stable amplitude variations (Selley et al., 2021; Strozzi et al., 2002; Surawy-Stepney et al., 2023a; Wallis et al., 2023). Feature tracking was performed using the GAMMA software, with a window and step size of three window sizes of 256x64, 362x144 and 400x160 range and azimuth pixels, each with a step size of approximately 25 % of the window size, after image co-registration using precise (5 cm error) orbit ephemerides and a 1x1 km Digital Elevation Model (DEM) (Bamber et al., 2009). Errors in the velocity measurements are caused by errors in the auxiliary DEM, imprecise co-registration of the SAR images, uncertainty in locating the cross-correlation peak and atmospheric delay due to variations in tropospheric water vapour and the ionosphere (Hogg et al., 2017; Nagler et al., 2015). We produce a spatially varying error estimate for each image-pair by dividing the ice speed by the signal-to-noise ratio of the cross-correlation function for each pixel (Lemos et al., 2018). The largest errors (> 30 %) occur at the rapidly deforming and highly crevassed shear margins and near each ice front, however, the centre of the major flow units typically have a lower relative error (Fig. S3).

For each image pair, we generate a signal-to-noise ratio-weighted mean velocity field of all available cross-correlation window sizes after removing outliers in the 2-D velocity fields. To remove outliers in the velocity field generated using each window size, we first compare each speed field to a reference speed map (Mouginot et al., 2019); speed estimates more than four times greater or four times smaller than the reference map are considered outliers and removed. Secondly, velocity estimates with a signal-to-noise ratio (SNR) of less than 5.8 are removed (De Lange et al., 2007). Third, flow directions more than 45 degrees different from the reference map are considered outliers and removed. Finally, we use a hybrid median filter with a 3x3 moving window, which replaces central pixels with the median of the central pixel, horizontally and vertically connected pixels, and diagonally connected pixels. Hybrid median filtering is designed to remove salt and pepper noise whilst preserving edges more

effectively than a traditional kernel-based median filter. We generate 100x100 m annual ice speed and ice speed error maps,
from 2015 to 2022, by mosaicking and averaging the image-pair speed and speed error estimates in each calendar year, in
which each image pair is weighted by its SNR. Prior to annually averaging, we remove temporal outliers from the time series
in two stages. First, we remove pixels more than 5 scaled Median Absolute Deviations (MAD) from the time-series median;
we then repeat this filter with a threshold of 2. Secondly, we remove local time-series outliers, defined as speed estimates more
than 3 scaled MADs from the local median in a 7-pixel moving window (approximately 6 weeks). After forming each annual
mosaic, we further remove spatial outliers in two stages. First, we remove spatially isolated pixel groups, defined as contiguous
regions of fewer than 100 pixels. Secondly, we remove pixels with unrealistically rapid changes in flow direction and speed,
defined as pixels in which the flow direction differs by more than 35 degrees, or the speed differs by more than 2 standard
deviations, from the median of the surrounding pixels in a 5x5 kernel. Finally, we perform a second filter based on 8-directional
speed gradients, where small (<1 km^2) regions enclosed by large speed gradients (more than 50 m yr^{-1} over 100 m (1-pixel))
are removed.

We used the MEaSUREs 1x1 km Antarctic annual ice velocity data (Mouginot et al., 2017) to calculate the longer-term rate
of ice speed change from 2005. This dataset was generated from a combination of SAR and optical imagery acquired over the
period 01.06.2005 to 31.05.2017, using both intensity tracking and interferometric techniques (Mouginot et al., 2017) (Table
S2). Combined with our new speed measurements, this study presents a 17.5-year long record of ice speed measurements from
June 2005 to December 2022 (Fig. S3).

2.2 Change in Calving Front Location and Ice Shelf Rifts

We measured the annual calving front location of the Crosson and Dotson Ice Shelves from 2009 to 2019 using Moderate
Resolution Imaging Spectroradiometer (MODIS) imagery (Andreasen et al., 2023). Images were acquired from mid-January
to the end of February to ensure consistent temporal sampling, and the calving fronts were manually delineated (Cook et al.,
2005; Cook and Vaughan, 2010). The uncertainty of the calving front location measurement is limited by the accuracy with
which the boundary can be delineated and the accuracy of the image georeferencing. Annual ice shelf area measurements were
calculated by using the annual calving fronts to modify a reference ice shelf mask (Rignot et al., 2011). To quantify any
changes in the Crosson Ice Shelf, we measured the area where the calving front location extends inland of the compressive
arch location from Lilien et al. (2018) assuming that the arch position is static throughout our study period. We also manually
delineated a persistent, long (~12 km) ice shelf rift near Bear Peninsula using the Sentinel-1 amplitude images and calculated
the distance between the rift tip's end and Bear Island's easternmost point (Fig. 1e).

3 Results

3.1 Ice Velocity

Our ice speed measurements show that, of the 8 major flow units in the PSK region, 6 ice streams reached mean speeds of over 700 m/yr in 2022 and with fast flowing ice streams penetrating up to ~75 km inland of the grounding line (Fig. 1a). For time series analysis, we extract ice speed measurements along flowline transects located on the fast-flowing central trunk of all 8 ice streams (Fig. 1a and Fig. 2) and compute grounding zone time-series averaging within 2.5 km diameter circles where the flow lines intersect with the grounding line. The fastest flowing ice streams are in the centre of the PSK region, where Kohler East, Smith West, and Smith East Glaciers flow at speeds up to 1,215 ± 275 m/yr (Table 1, Fig. 2). Relatively slower-moving ice is transported to the west of the inland Kohler Range through Kohler West and Horrall Glaciers, which respectively flow at speeds of 715 ± 319 m/yr and 401 ± 173 m/yr at the grounding line in 2022. To the East of the Crosson Ice Shelf ice is discharged through Pope, Vane, and Haynes Glaciers which respectively flow at speeds of 772 ± 211 m/yr, 203 ± 93 m/yr and 810 ± 169 m/yr (Table 1).
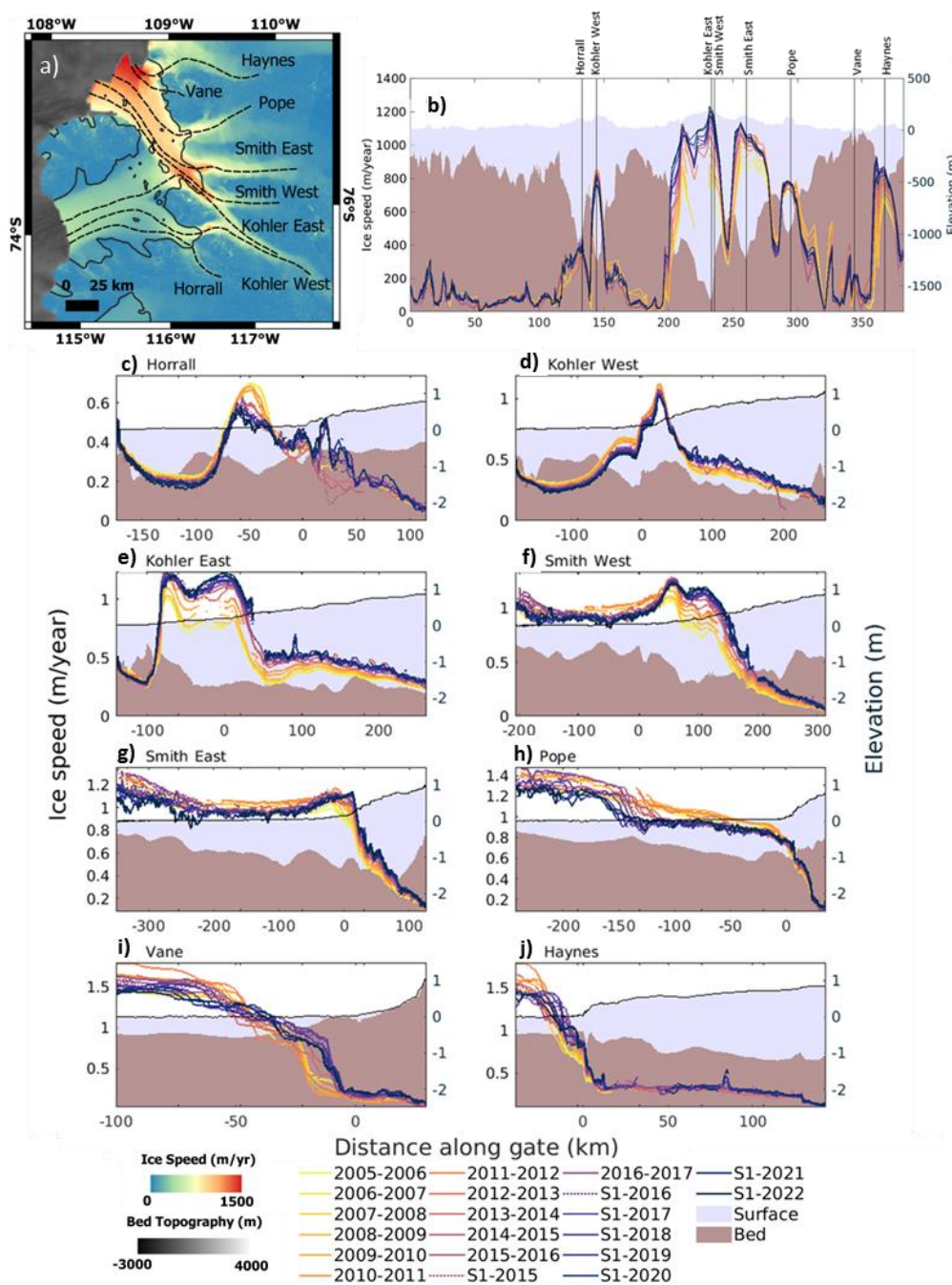
Figure 2: a) Average 2015 to 2022 ice speed over the PSK region, measured using interferometric Wide (IW) mode synthetic aperture radar (SAR) data acquired by the Sentinel-1a/b satellites. The 2011 grounding line location (solid black line) (Rignot et al., 2016) and the location of the 8 flow line profiles (dashed black lines) are also shown. b) Observed ice speed from 2005 to 2022 at the 2011 grounding line (Rignot et al., 2016) of Dotson and Crosson Ice Shelves in the Amundsen Sea Sector of West Antarctica. Also shown are the intersections of flow lines (black vertical lines), the bed topography (brown shading) and ice surface elevation and thickness (grey shading) from BedMachine (Morlighem et al., 2017). Observed speed along the flowlines c) Horrall d) Kohler West, e) Kohler East, f) Smith West, g) Smith East, h) Pope, i) Vane and j) Haynes.

Table 1: The observed mean ice speed in 2020, rate of speed change 2005-2020 and during the Sentinel-1 period (2015-2020) and the percentage speedup for both periods and rate of surface elevation change (1992-2023) (Shepherd et al., 2019) for the 8 major ice streams in the PSK region.

Region	Ice Stream Name	Mean Ice Speed in 2022 (m/yr)	Rate of speed change 2005-2022 (m/yr²)	Rate of speed change for Sentinel-1 period (2015-2022) (m/yr²)	Speed change from 2005-2022 (%)	Speed change in Sentinel-1 period (2015-2022) (%)	Rate of Surface Elevation Change (m/yr)
Western	Horrall	401 ± 173	2	4	10	9	-0.8
	Kohler West	715 ± 319	-5	-2	-10	-3	-1.1
Central	Kohler East	1215 ± 275	32	7	84	5	-2.5
	Smith West	1188 ± 253	32	11	87	8	-2.6
	Smith East	1093 ± 416	14	0	30	0	-2.7
Eastern	Pope	772 ± 210	3	1	7	1	-2.2
	Vane	203 ± 93	5	5	76	22	-0.9
	Haynes	810 ± 169	17	10	60	11	-1.1

3.2 Change in Ice Speed

We used our ice velocity measurements to calculate the overall change in ice speed from 2005 to 2022 across the PSK region. Speed change was calculated by fitting a linear trend through the ice speed time series in each pixel (Fig. 1b and 1c). We exclude pixels with fewer than 5 annual velocity estimates and retain speed change estimates where the fit was significant ($p < 0.05$) (Selley et al., 2021). Our results show that 7 ice streams in the study region have sped up since 2005, with 4 of those ice streams speeding up by over 60 % at the grounding line (Table 1). We observe the largest percentage increase in ice speed at the grounding zone of Smith West Glacier, where the rate of ice flow increased by 87 % over the 17.5-year study period reaching speeds of 1.2 km/yr by 2022 (Fig. 3a and Table 1). The fastest absolute rate of speed change was observed on Kohler East and Smith West Glacier where ice speeds respectively increased by 31.7 m/yr² and 31.5 m/yr² from 2005 to 2022 (Table 1). High rates of speed change are also observed on Haynes (17.4 m/yr²) and Smith East (14.3 m/yr²) Glaciers (Table 1); the central region containing Kohler East, Smith West, and Smith East Glaciers, accounts for 74 % of all the observed speed-up at the grounding line (Fig. 1).

145 Our results show that there is significant spatial variability in the observed speed change signal across the PSK region, and that change on individual ice streams has not been linear throughout the 17.5-year study period. In the Central and Eastern regions of PSK, although ice flow has sped-up throughout the study period, the rate of speed-up since 2015 was lower than that observed in the preceding decade between 2005 and 2015 (Table 1). In contrast, ice flow on Kohler West Glacier was 10 % slower in 2022 relative to its 2005 ice speed, with the slowdown starting around 2012. The western side of the Dotson Ice

150 Shelf into which these ice streams flow into has also decelerated by -4.8 m/yr² since 2005 (Fig. 1a and b). On Kohler West Glacier, the rate of ice flow slow-down has increased by 1.5 times since 2015 compared to the 2005 to 2015 mean (Table 1).

In addition to these long-term trends, we find all ice streams in the PSK region exhibit clear short-term speed variability around their 17.5-year trend (Fig. 3). This short-term variability is characterised by a period of rapid speed-up on all ice streams,

155 excluding Kohler West Glacier, from 2005 to 2010 and from 2014 to 2017, albeit minimal for Horrall Glacier. These speed-up episodes were separated by periods of steady or decelerating ice flow from 2011 to 2013 and from 2017 to the end of the study period in 2022 (Fig. 3a). There is some variability in the timing of these speed variations across the PSK region: slow-down begins later (2013) at Vane Glacier and is more prolonged at Pope Glacier (2012-2015), whilst the overall slow-down of Kohler West Glacier also began around 2012 but was sustained throughout the remainder of the study period.
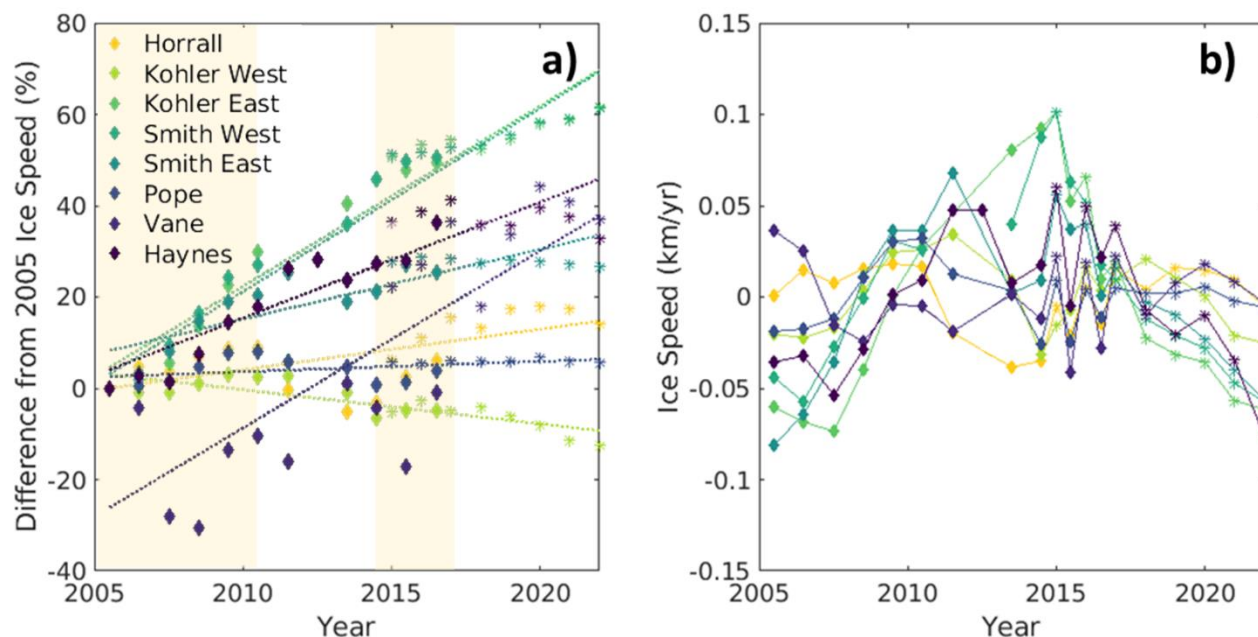
Figure 3: Observed relative speed change on 8 major ice streams in PSK over the 15-year study period. (A) Percentage change in speed from 2005 to 2022, from MEaSUREs (diamonds) (Mouginot et al., 2014) and Sentinel-1 (asterisks) velocity data, calculated as the difference in speed from the 2005 measurement. All measurements were extracted from a 2.5-km-diameter region where the central flow line crosses the grounding line (Fig. 1a) (Rignot et al., 2016). **(B)** De-trended annual

ice speeds for each of the 8 glaciers from 2005 to 2022, from MEaSUREs (diamonds) and Sentinel-1 (asterisks) velocity data, calculated as the difference in speed from the 2005 measurement. All measurements were extracted from a 2.5-km-diameter region where the central flow lines (Fig. 1a) cross the grounding line (Rignot et al., 2016).

160 **3.3 Redirection of Ice Flow**

Our ice velocity measurements reveal a substantial change in the direction of ice flow on two ice streams in the PSK study region (Fig. 4, S1 and Table S1), with three key changes in flow structure being especially notable. Firstly, at the division between Kohler West Glacier and Kohler East Glacier, we observe an eastward rotation of the ice flow vectors by 2019 (Fig. 4). Examination of ice flowlines generated from velocity measurements further show that this rotation results in redirection of

165 ice flow from Kohler West Glacier into Kohler East Glacier, which we interpret as a form of 'ice piracy' resulting from the differential rates of surface lowering observed at this ice stream division (Fig. 4). Secondly, we observe a westward rotation of the flow vectors in the region just downstream of the grounding lines of Kohler East and Smith West Glaciers, indicative of increased routing of ice into Dotson Ice Shelf that had previously fed the Crosson Ice Shelf (Fig. 4). Thirdly, the ice divide between Dotson and Crosson Ice Shelves has migrated eastwards within the study period (Fig. 4). These changes in flow

170 direction have had an impact on the advection of ice from Kohler West and Kohler East into Dotson and Crosson Ice Shelves, resulting in increased flux into Dotson and a smaller increase in flux to Crosson than would have been the case had flow directions remained stable (Fig. 4). These changes in flow direction are consistent with the observed changes in surface elevation and ice thickness in this region and would be expected to occur elsewhere in places where the geometry permits. Analogous historical changes in flow direction and ice divide migration have been inferred from chemical tracers (Iizuka et

175 al., 2010) and are widely documented in paleo ice sheet reconstructions (Conway and Rasmussen, 2009; Iizuka et al., 2010), whilst ongoing ice divide migration has been inferred from isochrones (Nereson et al., 1998) and thickness change measurements (Conway and Rasmussen, 2009). To our knowledge, however, redirection of ice flow from one ice stream to another has not been observed directly on ~15-year timescales, it may have occurred at glacier and ice cap scale. Differential thinning near ice stream boundaries is not isolated to this study region; therefore, we expect that ice divide migration and the

180 associated changes in flow direction have and will occur elsewhere in Antarctica, and this should be considered when interpreting observed changes in ice speed and ice thickness in tightly connected regions.
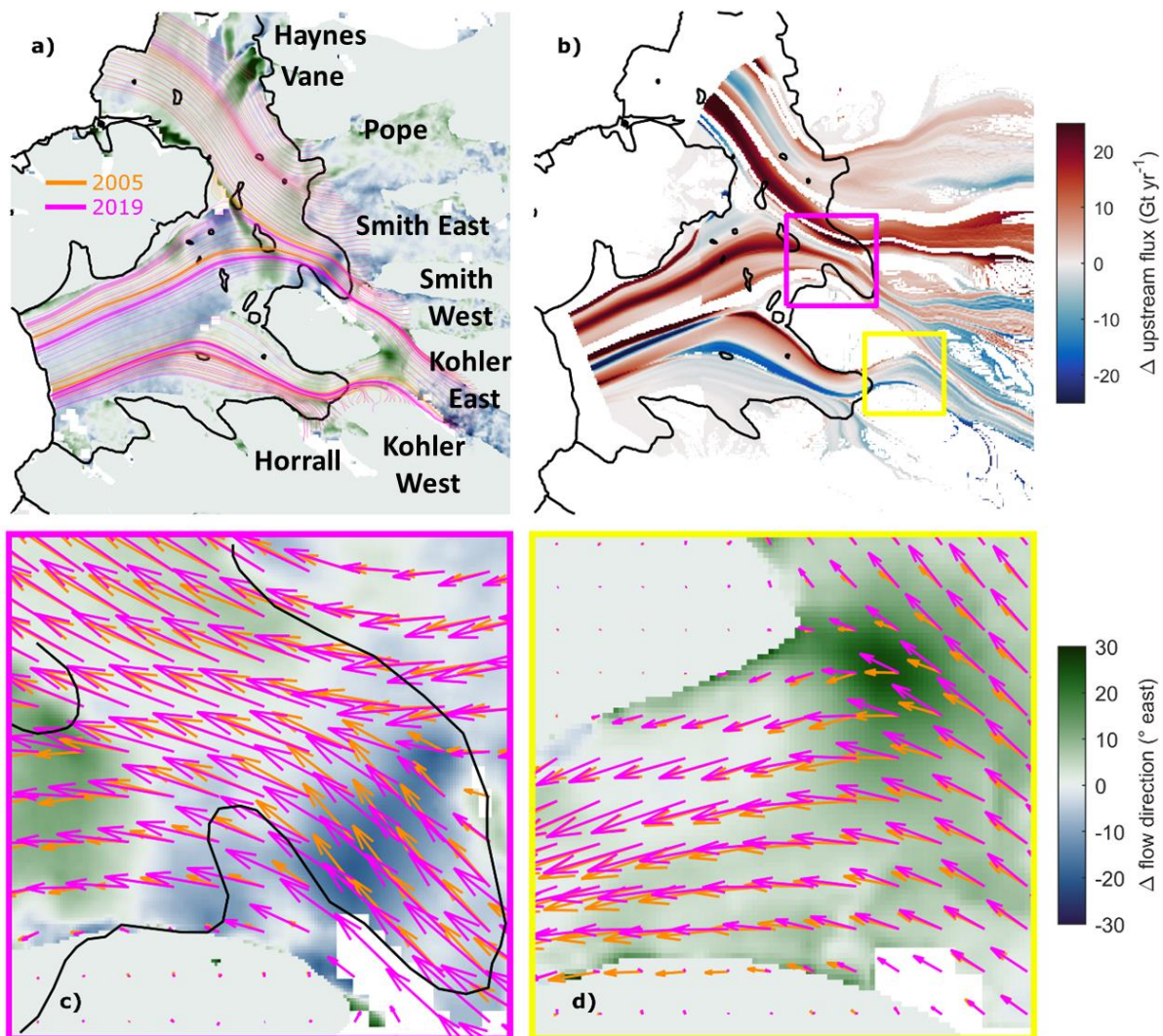
Figure 4: Flow lines and direction changes in the central Pope, Smith and Kohler Region. (A) Flow lines at the grounding line of the central PSK region for 2005 (orange) and 2019 (pink). Flow direction change (colour shading), and the grounding line location (solid black line) (Rignot et al., 2016) are also shown. **(B)** Change in downstream flux 2019 compared to 2005 calculated and displayed cumulatively along the flowlines from inland to the calving front, which indicates where ice mass is predominantly being directed on the ice shelves. Calculated using a time-varying ice thickness drawing on elevation change observations (Shepherd et al., 2019). Panels **(C)** and **(D)** show flow direction change and flow vectors in sub-regions near **(C)** the grounding line of Kohler East Glacier and **(D)** the division between Kohler West and Kohler East.

11

3.4 Change in Calving Front Location and Ice Shelf Rift Growth

Our measurements of the Dotson Ice Shelf calving front location show that the ice edge has remained in a relatively constant position throughout the study period, with a small (~4 km) but constant advance of its eastern limit until 2021 and a slight (~5 km) retreat in the west from 2005 to 2022 (Fig. 4). In contrast, the calving front of Crosson Ice Shelf has undergone several phases of retreat since 2005, the largest of which occurred in the period between 2013 and 2014. Overall, the calving front retreated by ~60 km, losing a ~85 km² area inland of the 1996 compressive arch at the eastern shelf edge and becoming heavily crevassed. During the same period as these large calving events, a 5 km rift formed at the eastern margin of the Crosson Ice Shelf and grew to ~12 km across the width of the ice shelf towards Bear Island during the study period (Fig. 5b, S1and S2). The distance between the end of the rift and Bear Island decreased from 8 km in 2015 to 5 km in 2022, with the rate of rift growth slowing from 2016 to 2022. The substantial increase in damage on the Crosson Ice Shelf inland of the compressive arch will have reduced the buttressing strength provided by the ice shelf, contributing to the observed speed-up of the glaciers that drain into it (Fig. 5).
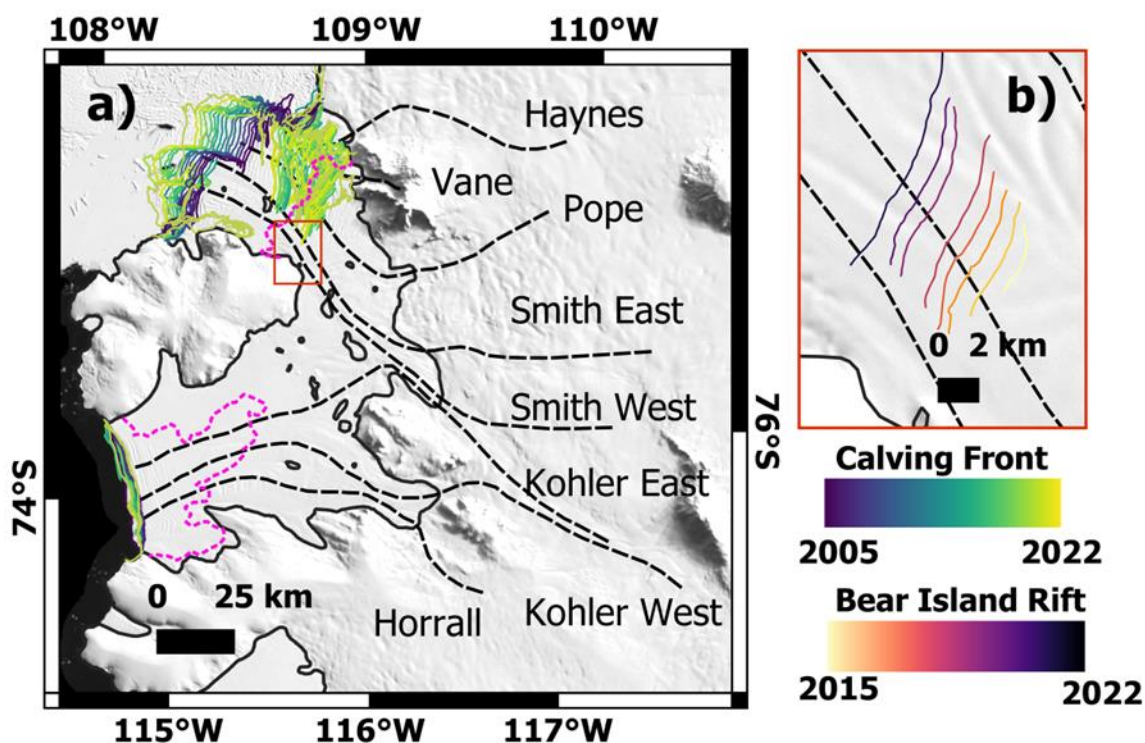
Figure 5: Dotson and Crosson Ice Shelf calving front and rift location. **(A)** Dotson and Crosson Ice Shelf calving front locations from 2005 to 2022 and the compressive arches (dotted pink line) (Lilien et al., 2018), are shown superimposed on the MODIS mosaic (Scambos et al., 2007). **(B)** Location of the rift approaching bear island through the Sentinel-1 period (2015-2022).

4 Discussion

Overall, our results extend the record and show a long-term speed-up at most major ice streams in the PSK study region
205   from 2005 to 2022, with an average speed increase at the grounding line of 51 %. Previous work focuses on the longer-term
changes back to the 1970s (Mouginot et al., 2014); here we focus on the short-term changes visible from the annual records
available from 2005. Although speed-up is greatest at the grounding line (Mouginot et al., 2014) it also extends up to ~100
km inland (Fig. 1b, 1c), impacting a substantial portion of the West Antarctic Ice Sheet. The zone of highest relative speed-
up is located inland of Bear Island on Smith West Glacier where the ice is thickest (Lilien et al., 2018), the bedrock is
210   deepest (Schoof, 2007) and where the grounding line has retreated the most (Konrad et al., 2017) (Table 1, Fig. 1b, 1c and
Fig. 2). During their overlapping periods, our observations of speed change closely agree with previous studies in terms of
the magnitude and spatial patterns of speed change (Lilien et al., 2018; Miles et al., 2022; Mouginot et al., 2014; Scheuchl
et al., 2016), which are consistent with observed patterns of grounding line retreat (Rignot et al., 2014) and surface elevation
change (McMillan et al., 2014). Our examination of individual ice stream behaviour and our addition of more recent
215   observations add further detail to our understanding of the evolution of the PSK region.

In addition to the long-term speed up, we observe shorter-term ice speed variability superimposed on the long-term speed-up
of most glaciers in the study region. We note periods of rapid speed-up 2005 to 2011 with an average speed difference across
all ice streams of 14 % and during 2014-2017 (12 %) were interrupted between 2011-2013 (4 %) and 2017-2020 (2 %) (Fig.
220   3a); the timing and relative magnitude of these speed fluctuations vary between ice streams, but the absolute magnitude of the
speed change is similar across the region (Fig. 1). Similar ice speed variability during these periods has previously been
documented at Pope Glacier, Kohler West Glacier, and Pine Island Glacier (Lilien et al., 2018; Mouginot et al., 2014; Scheuchl
et al., 2016). At Pine Island Glacier, this ice speed variability is attributed to fluctuations in the depth of the thermocline on
the continental shelf (Assmann et al., 2013; Dotto et al., 2019; Walker et al., 2007; Webber et al., 2017). Until 2014, the
225   shorter-term speed variability at PSK was broadly synchronous with those observed at Pine Island Glacier, implying that the
thermocline depth changes and the associated changes in oceanic heat delivery to ice shelf grounding lines during those times
were widespread in the Amundsen Sea Embayment, consistent with hydrographic surveys (Jenkins et al., 2018) and numerical
ocean modelling (Naughten et al., 2022a). Pine Island Glacier has rapidly sped up since 2017 (Davison et al., 2023; Joughin
et al., 2021), whereas in PSK rates of speedup have slowed or ice speeds have plateaued (Fig. 3). This may reflect the increased
230   role of calving and damage (Lhermitte et al., 2020; Surawy-Stepney et al., 2023b) on the recent speed changes observed at
Pine Island Glacier (Joughin et al., 2021).

In contrast to the rest of the region, Kohler West Glacier did not speed up appreciably after 2013, resulting in a moderate (~10
%) slowdown since 2012. The lack of significant speed-up of Kohler West Glacier has been attributed to the prograde bed
235   slope on which the grounding line rests (Milillo et al., 2022), making the ice stream less susceptible to ice dynamic change
and instability. Indeed, 18 m of thinning and a 0.03-degree decrease in ice surface slope (comparable to those observed on
Kohler West) would cause an 82 m/yr decrease in ice velocity, which is similar to the observed slow-down from 2005 to 2020

(Equation S1, Cuffey and Paterson, 2010). In conjunction with this deceleration of Kohler West, we observe redirection of ice flow from Kohler West Glacier into Kohler East Glacier (Fig. 4). We suggest that this so-called 'ice piracy' results from

240 the differential thinning rates of Kohler West (less than 2 m/yr) and Kohler East Glaciers (up to 9 m/yr) over the last few decades (McMillan et al., 2014; Nilsson et al., 2022). Modelling work indicates that minor changes in ice sheet geometry can result in 'ice piracy' and highlights the importance of quantifying the rates of change and subsequent impact on ice mass loss (McCormack et al., 2023).

245 The observed changes in flow speed and flow direction have downstream consequences for Dotson and Crosson Ice Shelves. The slow-down of Kohler West Glacier has reduced the ice flux into Dotson Ice Shelf by 0.68 Gt (11 %) locally from 2011 to 2022 (Fig. 4b). However, the discharge from Kohler East Glacier into the eastern part of Dotson Ice Shelf increased by 5.6 Gt (26 %) over the same time period because of the acceleration of Kohler East Glacier and because of the eastward migration of the ice divide between Dotson and Crosson Ice Shelves. We suggest that the divide migration between Dotson and Crosson

250 Ice Shelves has been instrumental in maintaining the apparent stability of the Dotson Ice Shelf, despite the slow-down of Kohler West Glacier. In contrast, Crosson Ice Shelf deteriorated substantially during our study period, characterised by rapid thinning and extensive crevassing, which we suggest has been exacerbated by the redirection of ice from Kohler East due to the ice shelf divide migration.

255 Some previous research has suggested that the rapid grounding line retreat and acceleration in the PSK region is indicative, if not diagnostic, of MISI (Milillo et al., 2022). At Pine Island Glacier, the rapid reduction in ice velocity in response to the lowering of the thermocline and presumably reduced basal melt rates has been used as evidence to suggest that MISI is not underway, or at least is conditional upon continued ocean forcing (Christianson et al., 2016). Similarly, recent modelling efforts suggest that the current grounding line positions in the ASE are stable (Hill et al., 2023). The fluctuations in speed we observe

260 suggest that ice streams in this region are responding to changes in external forcing similarly to Pine Island Glacier and that MISI may also not be a major dynamical factor at short (decadal) timescales across the PSK region. However, we observe that ice streams on prograde and retrograde bed topography are responding with opposing speed change trends (Fig. 2). This indicates that bed geometry is a key control on processes driving speed changes. It is plausible that there is still an instability which could have been triggered on centennial scales. The speed variability is indeed superimposed on a longer-term speed-

265 up. This may be driven by a centennial trend of ocean warming on the continental shelf (Naughten et al., 2022b), likely driven by a trend in winds over the continental shelf break (Holland et al., 2019, 2022), or it could be driven by internal ice dynamic feedbacks (such as MISI) or ice-ocean feedbacks, such as changes in cavity circulation due to ice shelf thinning and grounding line retreat (Bradley et al., 2022).

5 Conclusions

270 Our 17.5-year-long record of ice speed shows continued speed-up on the majority of ice streams in the Pope, Smith and Kohler catchment of West Antarctica, slow-down on two ice streams and previously unreported changes in flow direction and ice

divide locations. We measure concentrated regions of speed-up (51 % on average) at the grounding lines of Kohler East, Smith West and Smith East Glaciers since 2005. In contrast, Kohler West slowed down by 10 % over the 17.5-year period, with most of this occurring since 2012. This is potentially due to thinning-induced reductions in driving stress. Superimposed on these

275 speed change trends is a notable and widespread shorter-term periodicity, which is likely driven by variations in the depth of the thermocline in the ocean water on the continental shelf, comparable to that observed in the vicinity of Pine Island Glacier. In addition to these speed changes, we also observe substantial ice flow reorganisation of both grounded and floating ice. This has been characterised by 1) redirection of ice flow from Kohler West into Kohler East Glacier, which we attribute to differential thinning of the two ice streams, and 2) migration of the ice divide between Dotson and Crosson Ice Shelves, which

280 has resulted in redirection of ice flow from Kohler East and Smith West Glaciers into Dotson Ice Shelf from Crosson. These changes in flow direction have substantially altered the mass flux into Dotson and Crosson Ice Shelves, likely playing an important role in maintaining Dotson Ice Shelf and accelerating the deterioration of Crosson Ice Shelf. This suggests that ice flow redirection is an important component of contemporary ice sheet dynamics which is required to understand the recent structural change in Dotson and Crosson Ice Shelves, and which may affect their future evolution. Together, these observations

285 reveal previously undocumented interactions between the floating and grounded ice which will affect the future sea level contribution from the PSK region.

305

Author contributions:

Conceptualization: HLS, AEH

Methodology: HLS, BJD, TS

310   Investigation: HLS, BJD

Visualization: HLS, BJD

Supervision: AEH

Writing—original draft: HLS

Writing—review & editing: HLS, AEH, BJD, TS, PD

315

Competing interests: All other authors declare they have no competing interests.

Data and materials availability:

320   The annual ice speed mosaics, rate of ice speed change, calving fronts and Bear Island crack data will be made available from Pangaea upon publication.

References

Adusumilli, S., Fricker, H. A., Medley, B., Padman, L., and Siegfried, M. R.: Interannual variations in meltwater input to the Southern Ocean from Antarctic ice shelves, Nat Geosci, 1–5, https://doi.org/10.1038/s41561-020-0616-z, 2020.

325   Andreasen, J. R., Hogg, A. E., and Selley, H. L.: Change in Antarctic ice shelf area from 2009 to 2019, Cryosphere, 17, 2059–2072, https://doi.org/10.5194/TC-17-2059-2023, 2023.

Assmann, K. M., Jenkins, A., Shoosmith, D. R., Walker, D. P., Jacobs, S. S., and Nicholls, K. W.: Variability of Circumpolar Deep Water transport onto the Amundsen Sea Continental shelf through a shelf break trough, J Geophys Res Oceans, 118, 6603–6620, https://doi.org/10.1002/2013JC008871, 2013.

330   Bamber, J. L., Gomez-Dans, J. L., and Griggs, J. A.: A new 1 km digital elevation model of the Antarctic derived from combined satellite radar and laser data – Part 1: Data and methods, Cryosphere, 3, 101–111, https://doi.org/10.5194/tc-3-101-2009, 2009.

Bradley, A. T., Bett, D. T., Dutrieux, P., De Rydt, J., and Holland, P. R.: The Influence of Pine Island Ice Shelf Calving on Basal Melting, J Geophys Res Oceans, 127, e2022JC018621, https://doi.org/10.1029/2022JC018621, 2022.

335   Christianson, K., Bushuk, M., Dutrieux, P., Parizek, B. R., Joughin, I. R., Alley, R. B., Shean, D. E., Abrahamsen, E. P., Anandakrishnan, S., Heywood, K. J., Kim, T. W., Lee, S. H., Nicholls, K., Stanton, T., Truffer, M., Webber, B. G. M., Jenkins, A., Jacobs, S., Bindschadler, R., and Holland, D. M.: Sensitivity of Pine Island Glacier to observed ocean forcing, Geophys Res Lett, 43, 10,817-10,825, https://doi.org/10.1002/2016GL070500, 2016.

Iizuka, Y., Miura, H., Iwasaki, S., Maemoku, H., Sawagaki, T., Greve, R., Satake, H., Sasa, K., and Matsushi, Y.: Evidence of past migration of the ice divide between the Shirase and Sôya drainage basins derived from chemical characteristics of the marginal ice in the Sôya drainage basin, East Antarctica, Journal of Glaciology, 56, 395–404, https://doi.org/10.3189/002214310792447707, 2010.

Jenkins, A., Shoosmith, D., Dutrieux, P., Jacobs, S., Kim, T. W., Lee, S. H., Ha, H. K., and Stammerjohn, S.: West Antarctic Ice Sheet retreat in the Amundsen Sea driven by decadal oceanic variability, Nat Geosci, 11, 733–738, https://doi.org/10.1038/s41561-018-0207-4, 2018.

Joughin, I., Smith, B. E., and Holland, D. M.: Sensitivity of 21st century sea level to ocean-induced thinning of Pine Island Glacier, Antarctica, Geophys Res Lett, 37, https://doi.org/10.1029/2010GL044819, 2010.

Joughin, I., Smith, B. E., and Medley, B.: Marine ice sheet collapse potentially under way for the thwaites glacier basin, West Antarctica, Science (1979), 344, 735–738, https://doi.org/10.1126/science.1249055, 2014.

Joughin, I., Shapero, D., Smith, B., Dutrieux, P., and Barham, M.: Ice-shelf retreat drives recent Pine Island Glacier speedup, Sci Adv, 7, 3080–3091, https://doi.org/DOI: 10.1126/sciadv.abg3080, 2021.

Konrad, H., Gilbert, L., Cornford, S. L., Payne, A., Hogg, A., Muir, A., and Shepherd, A.: Uneven onset and pace of ice-dynamical imbalance in the Amundsen Sea Embayment, West Antarctica, Geophys Res Lett, 44, 910–918, https://doi.org/10.1002/2016GL070733, 2017.

Konrad, H., Shepherd, A., Gilbert, L., Hogg, A. E., McMillan, M., Muir, A., and Slater, T.: Net retreat of Antarctic glacier grounding lines, Nat Geosci, 11, 258–262, https://doi.org/10.1038/s41561-018-0082-z, 2018.

De Lange, R., Luckman, A., and Murray, T.: Improvement of satellite radar feature tracking for ice velocity derivation by spatial frequency filtering, IEEE Transactions on Geoscience and Remote Sensing, 45, 2309–2318, https://doi.org/10.1109/TGRS.2007.896615, 2007.

Lemos, A., Shepherd, A., McMillan, M., Hogg, A. E., Hatton, E., and Joughin, I.: Ice velocity of Jakobshavn Isbræ, Petermann Glacier, Nioghalvfjerdsfjorden, and Zachariæ Isstrøm, 2015-2017, from Sentinel 1-a/b SAR imagery, Cryosphere, 12, 2087–2097, https://doi.org/10.5194/tc-12-2087-2018, 2018.

Lhermitte, S., Sun, S., Shuman, C., Wouters, B., Pattyn, F., Wuite, J., Berthier, E., and Nagler, T.: Damage accelerates ice shelf instability and mass loss in Amundsen Sea Embayment, Proc Natl Acad Sci U S A, 117, 24735–24741, https://doi.org/10.1073/PNAS.1912890117/SUPPL_FILE/PNAS.1912890117.SM06.MP4, 2020.

Lilien, D. A., Joughin, I., Smith, B., and Shean, D. E.: Changes in flow of Crosson and Dotson ice shelves, West Antarctica, in response to elevated melt, Cryosphere, 12, 1415–1431, https://doi.org/10.5194/tc-12-1415-2018, 2018.

McCormack, F. S., Roberts, J. L., Kulessa, B., Aitken, A., Dow, C. F., Bird, L., Galton-Fenzi, B. K., Hochmuth, K., Jones, R. S., Mackintosh, A. N., and McArthur, K.: Assessing the potential for ice flow piracy between the Totten and Vanderford glaciers, East Antarctica, Cryosphere, 17, 4549–4569, https://doi.org/10.5194/TC-17-4549-2023, 2023.

McMillan, M., Shepherd, A., Sundal, A., Briggs, K., Muir, A., Ridout, A., Hogg, A., and Wingham, D.: Increased ice losses from Antarctica detected by CryoSat-2, Geophys Res Lett, 41, 3899–3905, https://doi.org/10.1002/2014GL060111, 2014.

Miles, B. W. J., Stokes, C. R., Jamieson, S. S. R., Jordan, J. R., Gudmundsson, G. H., and Jenkins, A.: High spatial and temporal variability in Antarctic ice discharge linked to ice shelf buttressing and bed geometry, Sci Rep, 12, 1–14, https://doi.org/10.1038/s41598-022-13517-2, 2022.

410   Milillo, P., Rignot, E., Rizzoli, P., Scheuchl, B., Mouginot, J., Bueso-Bello, J. L., Prats-Iraola, P., and Dini, L.: Rapid glacier retreat rates observed in West Antarctica, Nat Geosci, 15, 48–53, https://doi.org/10.1038/s41561-021-00877-z, 2022.

Morlighem, M., Rignot, E., Seroussi, H., Larour, E., Ben Dhia, H., and Aubry, D.: A mass conservation approach for mapping glacier ice thickness, Geophys Res Lett, 38, https://doi.org/10.1029/2011GL048659, 2011.

Mouginot, J., Rignot, E., and Scheuchl, B.: Sustained increase in ice discharge from the Amundsen Sea Embayment, West

415   Antarctica, from 1973 to 2013, Geophys Res Lett, 41, 1576–1584, https://doi.org/10.1002/2013GL059069, 2014.

Mouginot, J., Rignot, E., Scheuchl, B., and Millan, R.: Comprehensive Annual Ice Sheet Velocity Mapping Using Landsat-8, Sentinel-1, and RADARSAT-2 Data, Remote Sens (Basel), 9, 364, https://doi.org/10.3390/rs9040364, 2017.

Mouginot, J., Rignot, E., and Scheuchl, B.: Continent-Wide, Interferometric SAR Phase, Mapping of Antarctic Ice Velocity, Geophys Res Lett, 46, 9710–9718, https://doi.org/10.1029/2019GL083826, 2019.

420   Nagler, T., Rott, H., Hetzenecker, M., Wuite, J., and Potin, P.: The Sentinel-1 Mission: New Opportunities for Ice Sheet Observations, Remote Sens (Basel), 7, 9371–9389, https://doi.org/10.3390/rs70709371, 2015.

Naughten, K. A., Holland, P. R., Dutrieux, P., Kimura, S., Bett, D. T., and Jenkins, A.: Simulated Twentieth-Century Ocean Warming in the Amundsen Sea, West Antarctica, Geophys Res Lett, 49, e2021GL094566, https://doi.org/10.1029/2021GL094566, 2022a.

425   Naughten, K. A., Holland, P. R., Dutrieux, P., Kimura, S., Bett, D. T., and Jenkins, A.: Simulated Twentieth-Century Ocean Warming in the Amundsen Sea, West Antarctica, Geophys Res Lett, 49, e2021GL094566, https://doi.org/10.1029/2021GL094566, 2022b.

Nereson, N. A., Raymond, C. F., Waddington, E. D., and Jacobel, R. W.: Migration of the Siple Dome ice divide, West Antarctica, Journal of Glaciology, 44, 643–652, https://doi.org/10.3189/S0022143000002148, 1998.

430   Nilsson, J., Gardner, A. S., and Paolo, F. S.: Elevation change of the Antarctic Ice Sheet: 1985 to 2020, Earth Syst Sci Data, 14, 3573–3598, https://doi.org/10.5194/ESSD-14-3573-2022, 2022.

Paolo, F. S., Fricker, H. A., and Padman, L.: Volume loss from Antarctic ice shelves is accelerating, Science (1979), 348, 327–331, https://doi.org/10.1126/science.aaa0940, 2015.

Pritchard, H. D., Ligtenberg, S. R. M., Fricker, H. A., Vaughan, D. G., Van Den Broeke, M. R., and Padman, Laurie.: Antarctic

435   ice-sheet loss driven by basal melting of ice shelves, Nature, 484, 502–505, https://doi.org/10.1038/nature10968, 2012.

Rignot, E., Bamber, J. L., Van Den Broeke, M. R., Davis, C., Li, Y., Van De Berg, W. J., and Van Meijgaard, E.: Recent Antarctic ice mass loss from radar interferometry and regional climate modelling, Nat Geosci, 1, 106–110, https://doi.org/10.1038/ngeo102, 2008.

Rignot, E., Mouginot, J., and Scheuchl, B.: Antarctic grounding line mapping from differential satellite radar interferometry,

440   Geophys Res Lett, 38, https://doi.org/10.1029/2011GL047109, 2011.

Rignot, E., Mouginot, J., Morlighem, M., Seroussi, H., and Scheuchl, B.: Widespread, rapid grounding line retreat of Pine Island, Thwaites, Smith, and Kohler glaciers, West Antarctica, from 1992 to 2011, Geophys Res Lett, 41, 3502–3509, https://doi.org/10.1002/2014GL060140, 2014.

Rignot, E., Mouginot, J., and Scheuchl, B.: MEaSUREs Antarctic Grounding Line from Differential Satellite Radar

445   Interferometry, Version 2., Boulder, Colorado USA. NASA National Snow and Ice Data Center Distributed Active Archive Center. Available from: https://doi.org/10.5067/IKBWW4RYHF1Q, 02/04/2018, 2016.

Rignot, E., Mouginot, J., Scheuchl, B., Van Den Broeke, M., Van Wessem, M. J., and Morlighem, M.: Four decades of Antarctic ice sheet mass balance from 1979–2017, Proc Natl Acad Sci U S A, 116, 1095–1103, https://doi.org/10.1073/pnas.1812883116, 2019.

450   Scheuchl, B., Mouginot, J., Rignot, E., Morlighem, M., and Khazendar, A.: Grounding line retreat of Pope, Smith, and Kohler Glaciers, West Antarctica, measured with Sentinel-1a radar interferometry data, Geophys Res Lett, 43, 8572–8579, https://doi.org/10.1002/2016GL069287, 2016.

Schoof, C.: Ice sheet grounding line dynamics: Steady states, stability, and hysteresis, J Geophys Res Earth Surf, 112, https://doi.org/10.1029/2006JF000664, 2007.

455   Selley, H. L., Hogg, A. E., Cornford, S., Dutrieux, P., Shepherd, A., Wuite, J., Floricioiu, D., Kusk, A., Nagler, T., Gilbert, L., Slater, T., and Kim, T. W.: Widespread increase in dynamic imbalance in the Getz region of Antarctica from 1994 to 2018, Nat Commun, 12, 1–10, https://doi.org/10.1038/s41467-021-21321-1, 2021.

Shepherd, A., Ivins, E. R., Geruo, A., Barletta, V. R., Bentley, M. J., Bettadpur, S., Briggs, K. H., Bromwich, D. H., Forsberg, R., Galin, N., Horwath, M., Jacobs, S., Joughin, I., King, M. A., Lenaerts, J. T. M., Li, J., Ligtenberg, S. R. M., Luckman, A.,

460   Luthcke, S. B., McMillan, M., Meister, R., Milne, G., Mouginot, J., Muir, A., Nicolas, J. P., Paden, J., Payne, A. J., Pritchard, H., Rignot, E., Rott, H., Sørensen, L. S., Scambos, T. A., Scheuchl, B., Schrama, E. J. O., Smith, B., Sundal, A. V., Van Angelen, J. H., Van De Berg, W. J., Van Den Broeke, M. R., Vaughan, D. G., Velicogna, I., Wahr, J., Whitehouse, P. L., Wingham, D. J., Yi, D., Young, D., and Zwally, H. J.: A reconciled estimate of ice-sheet mass balance, Science (1979), 338, 1183–1189, https://doi.org/10.1126/SCIENCE.1228102/SUPPL_FILE/TABLES_S1_S3_S9_S10.XLSX, 2012.

465   Shepherd, A., Ivins, E., Rignot, E., Smith, B., Van Den Broeke, M., Velicogna, I., Whitehouse, P., Briggs, K., Joughin, I., Krinner, G., Nowicki, S., Payne, T., Scambos, T., Schlegel, N., Geruo, A., Agosta, C., Ahlstrøm, A., Babonis, G., Barletta, V., Blazquez, A., Bonin, J., Csatho, B., Cullather, R., Felikson, D., Fettweis, X., Forsberg, R., Gallee, H., Gardner, A., Gilbert, L., Groh, A., Gunter, B., Hanna, E., Harig, C., Helm, V., Horvath, A., Horwath, M., Khan, S., Kjeldsen, K. K., Konrad, H., Langen, P., Lecavalier, B., Loomis, B., Luthcke, S., McMillan, M., Melini, D., Mernild, S., Mohajerani, Y., Moore, P.,

470   Mouginot, J., Moyano, G., Muir, A., Nagler, T., Nield, G., Nilsson, J., Noel, B., Otosaka, I., Pattle, M. E., Peltier, W. R., Pie, N., Rietbroek, R., Rott, H., Sandberg-Sørensen, L., Sasgen, I., Save, H., Scheuchl, B., Schrama, E., Schröder, L., Seo, K. W., Simonsen, S., Slater, T., Spada, G., Sutterley, T., Talpe, M., Tarasov, L., Van De Berg, W. J., Van Der Wal, W., Van Wessem, M., Vishwakarma, B. D., Wiese, D., and Wouters, B.: Mass balance of the Antarctic Ice Sheet from 1992 to 2017, Nature, 558, 219–222, https://doi.org/10.1038/s41586-018-0179-y, 2018.

475 Shepherd, A., Gilbert, L., Muir, A. S., Konrad, H., McMillan, M., Slater, T., Briggs, K. H., Sundal, A. V., Hogg, A. E., and Engdahl, M. E.: Trends in Antarctic Ice Sheet Elevation and Mass, Geophys Res Lett, 46, 8174–8183, https://doi.org/10.1029/2019GL082182, 2019.

Smith, J. A., Andersen, T. J., Shortt, M., Gaffney, A. M., Truffer, M., Stanton, T. P., Bindschadler, R., Dutrieux, P., Jenkins, A., Hillenbrand, C. D., Ehrmann, W., Corr, H. F. J., Farley, N., Crowhurst, S., and Vaughan, D. G.: Sub-ice-shelf sediments

480 record history of twentieth-century retreat of Pine Island Glacier, Nature, 541, 77–80, https://doi.org/10.1038/nature20136, 2016.

Strozzi, T., Luckman, A., Murray, T., Wegmüller, U., and Werner, C. L.: Glacier motion estimation using SAR offset-tracking procedures, IEEE Transactions on Geoscience and Remote Sensing, 40, 2384–2391, https://doi.org/10.1109/TGRS.2002.805079, 2002.

485 Surawy-Stepney, T., Hogg, A. E., Cornford, S. L., and Davison, B. J.: Episodic dynamic change linked to damage on the Thwaites Glacier Ice Tongue, Nat Geosci, 16, 37–43, https://doi.org/10.1038/s41561-022-01097-9, 2023a.

Surawy-Stepney, T., Hogg, A. E., Cornford, S. L., and Hogg, D. C.: Mapping Antarctic crevasses and their evolution with deep learning applied to satellite radar imagery, Cryosphere, 17, 4421–4445, https://doi.org/10.5194/TC-17-4421-2023, 2023b.

490 Walker, D. P., Brandon, M. A., Jenkins, A., Allen, J. T., Dowdeswell, J. A., and Evans, J.: Oceanic heat transport onto the Amundsen Sea shelf through a submarine glacial trough, Geophys Res Lett, 34, https://doi.org/10.1029/2006GL028154, 2007.

Wallis, B. J., Hogg, A. E., van Wessem, J. M., Davison, B. J., and van den Broeke, M. R.: Widespread seasonal speed-up of west Antarctic Peninsula glaciers from 2014 to 2021, Nat Geosci, 16, 231–237, https://doi.org/10.1038/s41561-023-01131-4, 2023.

495 Webber, B. G. M., Heywood, K. J., Stevens, D. P., Dutrieux, P., Abrahamsen, E. P., Jenkins, A., Jacobs, S. S., Ha, H. K., Lee, S. H., and Kim, T. W.: Mechanisms driving variability in the ocean forcing of Pine Island Glacier, Nat Commun, 8, 1–8, https://doi.org/10.1038/ncomms14507, 2017.

Weertman, J.: Stability of the junction of an ice sheet and an ice shelf, Journal of Glaciology, 13, 3–11, https://doi.org/10.1017/S0022143000023327, 1974.

500 Zinck, A.-S. P., Wouters, B., Lambert, E., and Lhermitte, S.: Unveiling spatial variability within the Dotson Melt Channel through high-resolution basal melt rates from the Reference Elevation Model of Antarctica, Cryosphere, 17, 3785–3801, https://doi.org/10.5194/TC-17-3785-2023, 2023.